Membrane properties and spike generation in rat visual cortical cells during reversible cooling

Maxim Volgushev*†, Trichur R. Vidyasagar‡, Marina Chistiakova*†, Tagrid Yousef* and Ulf T. Eysel*

*Department of Neurophysiology, Faculty of Medicine, Ruhr-University Bochum, D-44780 Bochum, Germany, †Institute of Higher Nervous Activity and Neurophysiology Russian Academy of Sciences, 117865 Moscow, Russia and ‡Division of Psychology, Australian National University, Canberra, Australia

(Received 28 May 1999; accepted after revision 27 October 1999)

1. We studied the effects of reversible cooling between 35 and 7 °C on membrane properties and spike generation of cells in slices of rat visual cortex.

2. Cooling led to a depolarization of the neurones and an increase of the input resistance, thus bringing the cells closer to spiking threshold. Excitability, measured with intracellular current steps, increased with cooling.

3. Synaptic stimuli were most efficient in producing spikes at room temperature, but strong stimulation could evoke spikes even below 10 °C.

4. Spike width and total area increased with cooling, and spike amplitude was maximal between 12 and 20 °C. Repetitive firing was enhanced in some cells by cooling to 20–25 °C, but was always suppressed at lower temperatures.

5. With cooling, passive potassium conductance decreased and the voltage-gated potassium current had a higher activation threshold and lower amplitude. At the same time, neither passive sodium conductance nor the activation threshold of voltage-dependent sodium channels changed. Therefore changing the temperature modifies the ratio between potassium and sodium conductances, and thus alters basic membrane properties.

6. Data from two cells recorded in slices of cat visual cortex suggest a similar temperature dependence of the membrane properties of neocortical neurones to that described above in the rat.

7. These results provide a framework for comparison of the data recorded at different temperatures, but also show the limitations of extending the conclusions drawn from *in vitro* data obtained at room temperature to physiological temperatures. Further, when cooling is used as an inactivation tool *in vivo*, it should be taken into account that the mechanism of inactivation is a depolarization block. Only a region cooled below 10 °C is reliably silenced, but it is always surrounded by a domain of hyperexcitable cells.

Temperature is a factor that has a crucial influence on the functioning of nerve cells. Changing the temperature alters the basic properties of excitable cells, such as the membrane potential, the input resistance, the shape and amplitude of action potentials and the propagation of spikes. Recently it has been demonstrated that Ca^{2+} influx produced by an action potential in neocortical cells is larger at room temperature than in the physiological temperature range (Borst & Sakmann, 1998), and that transmitter spillover in the hippocampus is increased at room temperature (Kullmann & Asztely, 1998). So far, studies on the temperature dependence of membrane properties and synaptic transmission have been done mostly in invertebrates (Hodgkin & Katz, 1949; Gorman & Marmor, 1970; Westerfield *et al.* 1978) or lower vertebrates (Schoepfle & Erlanger, 1941; Frankenhaeuser & Moore, 1963). However, the properties of mammalian cells might depend on temperature in a quite different way, as for example in the case of Na^+ currents in frog and rabbit muscle cells (Kirsch & Sykes, 1987), or the ratio between sodium and potassium permeabilities, which increases with temperature in molluscan neurones (Gorman &

Marmor, 1970), but decreases in cat spinal motoneurones (Klee *et al.* 1974). Further, at temperatures around 36–38 °C a heat block of action potential propagation occurs in invertebrates (Hodgkin & Katz, 1949; Guttman, 1971), while for mammals this is the normal body temperature. These differences may not be surprising, since mammalian nerve cells might be adapted to perform best at around 36–38 °C, but the nerve cells of lower vertebrates and invertebrates need to work at lower temperatures and in a much wider range: from slightly above 0 °C to about 35 °C, rarely higher. Therefore, the results of experiments on invertebrates and lower vertebrates might have only limited implications for mammals.

Determining the mechanisms of the temperature dependence of the properties of mammalian neurones is important for both *in vivo* and *in vitro* studies. With the rapidly increasing interest in understanding the interactions between different cortical areas, cooling has become a widely used method of reversible local inactivation (see Payne *et al.* 1996 for review). Furthermore, cooling or warming by only a few degrees leads to a marked change in the amplitude of field potentials and dramatically alters the relationship between field EPSPs and population spikes in the hippocampus (Moser *et al.* 1993; Erickson *et al.* 1996). Therefore, an understanding of the processes that take place in a moderately cooled region and of the mechanisms of deactivation by cooling is necessary for interpretation of the results. *In vitro* studies on nerve membrane properties, synaptic transmission and its plasticity, properties of ionic channels, etc., have been performed at different temperatures, ranging usually from 20 to 35 °C. Therefore a quantitative characterization of the temperature dependence of the basic properties of the cell membrane is important both for interpretation and comparison of the results obtained at different temperatures as well as for making accurate inferences from *in vitro* data for physiological conditions.

The main purpose of our study was a quantitative description of a wide range of passive and active membrane properties and of spike generation in neocortical neurones at temperatures ranging from 7 to 35 °C and an analysis of the mechanisms underlying their temperature dependence. Part of these data has appeared in abstract form (Chistiakova *et al.* 1997).

METHODS

Slices

Slices of the visual cortex of 3- to 6-week-old Wistar rats (Charles River GmbH, Suzfeld, Germany) were prepared by conventional methods (Volgushev *et al.* 1998). The rats were anaesthetized with ether, decapitated and the brain rapidly removed and put into an ice-cold oxygenated solution. One hemisphere was mounted onto an agar block and 350–400 μm thick sagittal slices containing the visual cortex were cut with a vibratome (TSE, Kronberg, Germany) in ice-cold oxygenated solution. The slices were placed into an incubator where they recovered for at least 1 h at room temperature. After this time a slice was placed in the recording chamber. The solution used during the preparation of the slices had the same ionic composition as the recording medium (see below), but without L-glutamine. Slices of the cat visual cortex were prepared from brains obtained at the end of acute *in vivo* experiments in which one of the hemispheres remained intact. The animal was deeply anaesthetized by increasing halothane (Eurim-Pharm, Germany) concentration in a N_2O:O_2 (70:30) gas mixture to 3–3·5% and perfused with an ice-cold oxygenated solution with the same ionic composition as that used for slice preparation. The visual cortex of the intact hemisphere was exposed, and a block of tissue containing the visual cortex was cut, removed from the cat and put into ice-cold oxygenated solution. After this point, the procedures were the same as described above, except that thicker slices were cut (400–500 μm). The methods used in this study were in accordance with the guidelines published in the European Communities Council Directive (86/609/EEC, 1986) and were approved by a regional animal welfare committee (Arnsberg, Germany).

Recording and data analysis

Recordings were made with the slices in submerged conditions. The perfusion medium contained (mM): 125 NaCl, 2·5 KCl, 2 $CaCl_2$, 1 $MgCl_2$, 1·25 NaH_2PO_4, 25 $NaHCO_3$, 25 D-glucose and 0·5 L-glutamine, bubbled with 95% O_2 and 5% CO_2. To block sodium channels and isolate potassium currents in some experiments tetrodotoxin was added to the perfusion medium. The temperature in the recording chamber was varied within the range 7–35 °C and monitored with a thermocouple positioned close to the slice, 2–3 mm from the recording site.

Patch electrodes were filled with a potassium gluconate- or caesium methanesulfonate-based solution (mM: 127 potassium gluconate or caesium methanesulfonate, 20 KCl, 2 $MgCl_2$, 2 Na_2ATP, 10 Hepes and 0·1 EGTA with 0·3–1·0% biocytin) and had a resistance of 2–6 MΩ. Whole-cell recordings from pyramidal and non-pyramidal neurones in layers II–VI in slices of rat visual cortex were made under visual control using Nomarski optics and infrared videomicroscopy (Dodt & Zieglgänsberger, 1990; Stuart *et al.* 1993). Responses to current or voltage steps and to synaptic stimulation were recorded, while slowly cooling and re-warming the recording chamber. Synaptic responses were evoked by electric shocks applied through bipolar stimulation electrodes located 0·5–1·5 mm below or lateral to the recording site. The cells were recorded for periods ranging from 40 min to over 3 h in a bridge or a voltage-clamp mode; in some cells recordings in the two modes were made alternately. Some cells were recorded over several repetitive cooling and re-warming cycles. The stability of the recording situation was assured by the reversibility of temperature-induced changes and the similarity of the cell's responses recorded at the same temperature before and after cooling.

After amplification using Axoclamp-2A (Axon Instruments) and low-pass filtering at 5 kHz, both electrophysiological and temperature data were digitized at 10 kHz and fed into a computer (PC-486; Digidata 1200 interface and pCLAMP software, Axon Instruments). In some cases responses with very slow dynamics seen at temperatures below 15 °C were digitized at 5 kHz. Data were processed off-line using custom-written programs. Statistical analysis was based on Student's two-tailed t test and Wilcoxon-Mann-Whittney test. The differences were considered as significant at $P < 0·05$ if not stated otherwise. The data are presented as means ± S.E.M.

The EPSP amplitudes were measured as the difference between the mean membrane potential within two windows of 1–5 ms width, one positioned immediately before the response and the other one around the peak of the averaged EPSP, or on the last portion of the rising slope. The spike amplitudes were measured in two ways: from the origin of the regenerative process (spike threshold) and from the resting membrane potential to the peak. We have used both these measurements because of large depolarizing shifts of the resting membrane potential associated with cooling. The spike area was measured as the integral area under the curve from the spike origin to the moment when the amplitude after the peak exceeded the threshold by less than 15 mV.

Morphology

The tissue containing biocytin-labelled cells was processed as follows. Slices were fixed overnight in 2–4% paraformaldehyde containing 0·5% glutaraldehyde (E. Merck, Darmstadt, Germany) in 0·1 M phosphate buffer (pH 7·4) and cut into 60 μm sections on a freezing microtome. After several rinses in phosphate buffer and Tris-buffered saline (TBS, Tris buffer; Trizma base plus Trizma hydrochloride, pH 7·6, Sigma) the sections were incubated in avidin–biotin complexed with horseradish peroxidase (1:200, ABC, Vector Laboratories, Burlingame, CA, USA) diluted in TBS containing 0·05% Triton X-100 at 4 °C overnight. The sections were then rinsed in TBS followed by Tris, and incubated for the enzymatic reaction in 0·005% 3,3′-diaminobenzidine-4-HCl (Sigma) in TBS supplemented with $CoCl_2$ for intensification for 20 min. Hydrogen peroxide (final concentration, 0·00125%) was added to complete the enzymatic reaction. The sections were washed in TBS then phosphate buffer, and postfixed in 1% OsO_4 (Sigma) in phosphate buffer for 15–30 min, dehydrated and embedded in Durcupan ACM resin (Fluka, Neu-Ulm, Germany) on slides. Three-dimensional reconstruction was made using a ×100 oil objective and the Neurolucida system (MicroBrightField, USA).

Chemicals

The following chemicals were obtained from Sigma: biocytin, caesium methanesulfonate, EGTA, Hepes, potassium gluconate, L-glutamine, Na_2ATP and tetrodotoxin. The remaining chemicals were from J. T. Baker B.V. (Deventer, Holland) when not indicated otherwise.

RESULTS

Whole-cell recordings were made from different types of neurones in slices of the visual cortex of adult rats ($n = 32$ cells). Cells of a certain morphological type and location within the cortex were pre-selected using infrared videomicroscopy with contrast enhancement (Dodt & Zieglgänsberger, 1990). Some of the cells were injected with biocytin and their morphological type was verified. Of the 32 cells, 14 were layer 2–3 pyramidal cells, eight were layer 5 pyramidal cells and six were non-pyramidal cells comprising three spiny stellates from layer 4 and three aspiny (putative inhibitory) stellates. The remaining four cells were neither labelled nor could they be identified unambiguously during the recording. In addition to the rat data, we recorded from two layer 2–3 pyramidal cells in slices of cat visual cortex.

Passive membrane properties

A number of passive membrane properties – membrane potential, input resistance, total membrane conductance and partial potassium and sodium conductances – were estimated at different temperatures. All these parameters (except for partial sodium conductance) changed markedly upon lowering the bath temperature and recovered with re-warming.

Membrane potential. Membrane potential underwent dramatic but reversible changes during cooling and re-warming of the slice. Lowering the bath temperature led to a marked depolarization of the cell membrane. In the example in Fig. 1*A*, cooling the medium from 31 to 12 °C resulted in depolarization of the cell by about 30 mV. In the depolarized state reached around 15–12 °C, spontaneous spikes, followed by an extremely long (up to 200–300 ms) residual afterpolarization, sometimes occurred and interfered with membrane potential measurements (see several points lying well above the rest in the lower graph in Fig. 1*A*). During re-warming, membrane potential rapidly recovered and reached the value observed before cooling. Membrane potential showed a remarkably strong inverse correlation with temperature (Fig. 1*B*). In 18 out of 22 cells, the coefficient of correlation between the two parameters was lower than −0·9 (absolute value being higher than 0·9, $P \ll 0{\cdot}001$). Moreover, in these cells membrane potential had a nearly linear dependence on the temperature, as in Fig. 1*B*. For these cells, the gradient of the linear regression line, and hence the change of the membrane potential per degree Celcius, ranged from −1·03 to −2·21 mV °C^{-1}. However in the remaining four cells, the dependence of the membrane potential on temperature was quite different from linear. An extreme example of this kind is shown in Fig. 1*C*. In this cell, membrane potential was essentially independent of temperature in the interval from 36 to 20 °C. With further cooling below 20 °C the cell depolarized very rapidly (crosses in Fig. 1*C*). The same pattern of dependence of the membrane potential on temperature, but in a reverse order, was observed during re-warming of this cell (Fig. 1*C*, filled circles). Even in such cells with non-linear changes of the membrane potential with temperature, an overall correlation between the two parameters was strong and highly significant ($P \ll 0{\cdot}001$). In some cells (6 out of 22) a runaway depolarization (above −40 mV) accompanied by spiking was observed at temperatures below 12–15 °C. In such cases cooling was stopped and re-warming started, which led to a recovery of the membrane potential to initial values.

Input resistance. The cell input resistance was measured from responses to steps of hyperpolarizing current of a constant amplitude (in bridge mode) or to steps of the holding potential (in voltage-clamp mode) applied during cooling and re-warming of the recording chamber. In nearly two-thirds of all cases (18 out of 30), input resistance was estimated from the slope of the current–voltage

relationships measured at different temperatures. Input resistance, like the membrane potential, was strongly dependent on the temperature, increasing with cooling and decreasing back to the original values during re-warming of the slice (Fig. 2*A* and *B*). In a typical case shown in Fig. 2*A–C*, a linear dependence was observed between the input resistance and temperature, with an extremely high inverse correlation between these two parameters. A linear dependence and a highly significant ($P \ll 0{\cdot}001$) correlation were observed in the majority of cases (22 out of 30). In all but one cell input resistance increased upon lowering of the temperature with the gradient varying from $-0{\cdot}5$ to -16 MΩ °C^{-1}. In 25 out of 30 cells its absolute value was above 2 MΩ °C^{-1}. In eight cells after a typical increase of the input resistance with cooling, a decrease of the input resistance was observed at temperatures below 15–12 °C. This decrease was probably due to depolarization of the cell to the threshold level for activation of sodium conductances.

Temperature dependence of the membrane potential and input resistance in cells of different types. To evaluate whether individual differences between cells in the dependence of the membrane potential and the input resistance on temperature could be related to their morphological type, the data for layer 2–3 pyramidal cells, non-pyramidal cells from layers 2–4 and layer 5 pyramidal cells were compared. The membrane potential of layer 2–3 pyramidal cells at high temperatures (above 25 °C, $-77{\cdot}4 \pm 0{\cdot}6$ mV) was significantly different ($P < 0{\cdot}01$) from those of the non-pyramidal cells ($-68{\cdot}7 \pm 0{\cdot}9$ mV) and the layer 5 pyramidal cells ($-62{\cdot}4 \pm 2{\cdot}9$ mV). This difference persisted at lower temperatures, but was no longer statistically significant.

The input resistance was highest for the group of non-pyramidal cells (287 ± 21 MΩ at temperatures above 25 °C) compared to the layer 3 pyramidal cells (111 ± 14 MΩ) and layer 5 pyramidal cells (106 ± 12 MΩ). This difference remained significant at lower temperatures.

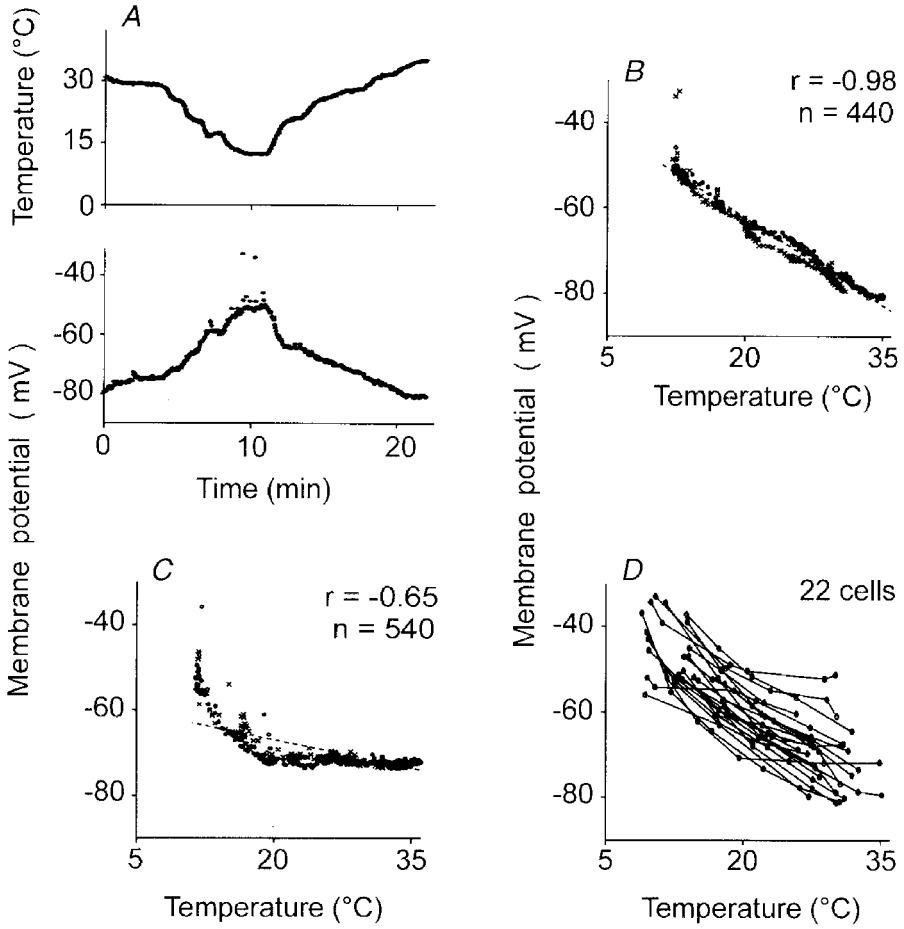

Figure 1. Dependence of the membrane potential on temperature

A, time course of changes of temperature in the recording chamber (upper graph) and of the membrane potential (lower graph) in a layer 2–3 pyramidal cell. *B*, scatter diagram showing dependence of the membrane potential on temperature; same data as in *A*. Values obtained during cooling are shown as crosses; those during re-warming are shown as filled circles. *C*, an exceptional example of a non-linear dependence of the membrane potential on temperature; same representation as in *B*. Data from a layer 4 spiny stellate cell. *D*, summary data. For each cell, temperature and membrane potential values were averaged within 5 °C intervals (circles) and connected with a line.

Despite the differences in the absolute values of the membrane potential and the input resistance, the dependence of these two parameters on temperature was similar in all cell types: with lowering of the temperature the membrane potential was depolarized and the input resistance increased. Therefore for further analysis, the cells were pooled.

Total membrane conductance and partial ionic conductances. To quantify the changes of the total membrane conductance and to estimate the possible contribution of partial ionic conductances to the total change, the data for each cell were subdivided into three temperature ranges: 11–18 °C, 18–25 °C and 25–32 °C. The mean membrane potential and resistance within each range, as well as the mean temperature at which the measurements in this range were performed, were calculated. Using these data, scatter diagrams showing the dependence of the membrane potential, input resistance and total membrane conductance on temperature were constructed, and the overall mean values were calculated.

As expected, a strong (Fig. 3*A*, top) and highly significant ($P < 0{\cdot}001$) negative correlation between the membrane potential and temperature was present in the whole sample. The mean gradient of the membrane potential changes was $-1{\cdot}3$ mV °C^{-1}. The mean values of the membrane potential were significantly different between any pair of temperature intervals (Fig. 3*A*, bottom). The overall correlation between the input resistance (Fig. 3*B*, top) or the membrane conductance (Fig. 3*C*, top) and the temperature was less pronounced, although also significant ($P < 0{\cdot}01$). A significant difference was found only between the mean values for the extreme temperature ranges, 11–18 *vs.* 25–32 °C (Fig. 3*B* and *C*, bottom). The significance level was low ($P < 0{\cdot}1$) when neighbouring intervals (11–18 *vs.* 18–25 °C and 18–25 *vs.* 25–32 °C) were compared.

For the cells for which data on changes of both the membrane potential and input resistance were available, it was possible to estimate the relative changes of partial ionic conductances using the

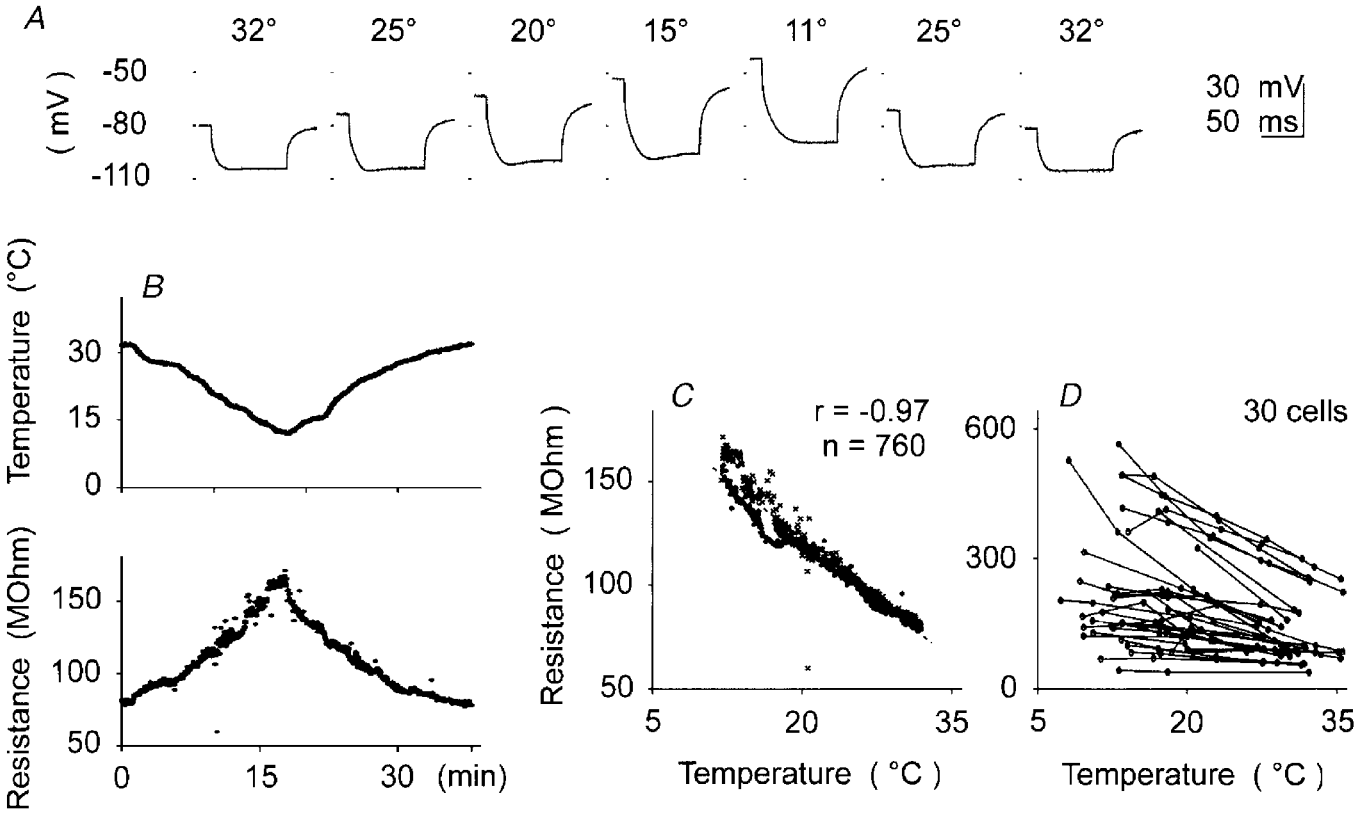

Figure 2. Dependence of the cell input resistance on temperature

A, responses of a layer 2–3 pyramidal cell to negative current steps (−0·3 nA, 100 ms) recorded at different temperatures (°C) during cooling and re-warming (as indicated). *B*, time course of changes of temperature in the recording chamber (upper graph) and of the input resistance in the same cell (lower graph). *C*, scatter diagram showing dependence of the input resistance on temperature; same data as in *B*. Values obtained during cooling are shown as crosses; those during re-warming are shown as filled circles. *D*, summary data. For each cell, temperature and input resistance values were averaged within 5 °C intervals (circles) and connected with a line.

Goldman-Hodgkin-Katz equations. The membrane potential can be described with the following equation (Hodgkin & Horowicz, 1959):

$$V_m = E_K \frac{P_K}{P_K + P_{Na} + P_{Cl}} + E_{Na} \frac{P_{Na}}{P_K + P_{Na} + P_{Cl}} + E_{Cl} \frac{P_{Cl}}{P_K + P_{Na} + P_{Cl}}, \quad (1)$$

where V_m is the membrane potential of a cell, E_K, E_{Na} and E_{Cl} are equilibrium potentials, and P_K, P_{Na} and P_{Cl} are membrane permeability for the respective ions.

In a whole-cell recording situation, intracellular concentrations of ions become equilibrated with the pipette solution within the first several minutes after rupturing the membrane (Neher & Sakmann, 1983), and reversal potentials for different ions can be calculated using the Nernst equation. With the ionic concentrations we used (see Methods), reversal potentials depended on temperature as follows:

$$E_K = \frac{RT}{F} \ln \frac{[K^+]_o}{[K^+]_i} = -0{\cdot}35Tm,$$

$$E_{Na} = \frac{RT}{F} \ln \frac{[Na^+]_o}{[Na^+]_i} = 0{\cdot}31Tm,$$

$$E_{Cl} = \frac{RT}{F} \ln \frac{[Cl^-]_o}{[Cl^-]_i} = -0{\cdot}15Tm,$$

where R is the gas constant, F is Faraday's constant, T is temperature (°K) and m is millivolts per degree Kelvin (mV °K^{-1}).

With these values, eqn (1) gives the following dependence of the membrane potential on temperature:

$$V_m(T) = \frac{-0{\cdot}35P_K + 0{\cdot}31P_{Na} - 0{\cdot}15P_{Cl}}{P_K + P_{Na} + P_{Cl}} Tm. \quad (2)$$

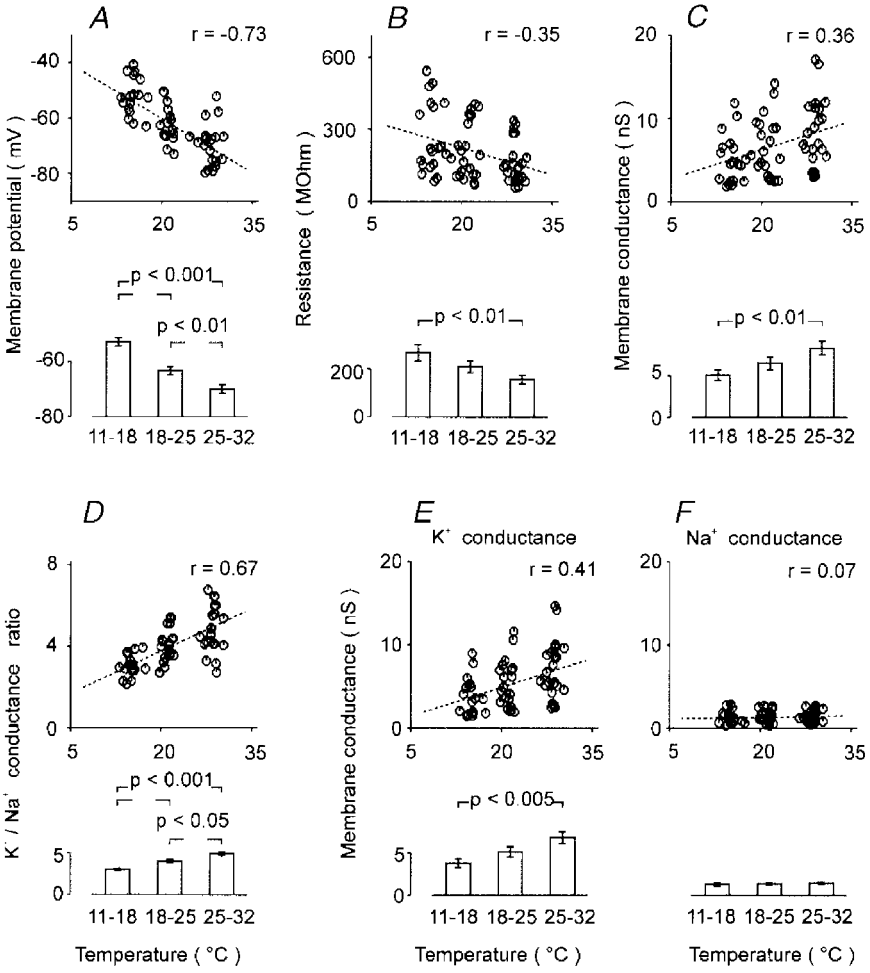

Figure 3. Estimations of changes of the membrane potential, input resistance and passive membrane conductance with temperature

For each cell, values of the membrane potential (*A*) and input resistance (*B*), as well as the temperature at which the measurements were made were averaged within the temperature ranges of 11–18 °C, 18–25 °C and 25–32 °C. These averaged values were used for constructing the scatter diagrams and for calculation of further parameters. The total membrane conductance (*C*) was calculated as 1/resistance (1/*R*). The ratio between K^+ and Na^+ conductances (*D*) was calculated using the Goldman-Hodgkin-Katz equations (see Results for details). Partial potassium (*E*) and sodium (*F*) conductances were calculated as their respective contributions multiplied by the total conductance (see Results for details). In *A*–*F*, scatter diagrams (top) show dependence of the parameter on temperature and correlation coefficient; bar histograms (bottom) show mean values for each temperature range and the significance of their difference.

It is clear from this equation that if the ratio between partial Na^+, K^+ and Cl^- conductances were constant and not affected by the temperature, changes of the equilibrium potentials with temperature could account for a membrane potential gradient of $-0{\cdot}35$ mV °C^{-1} in an extreme, purely theoretical case when both P_{Na} and P_{Cl} are equal to zero, but this gradient would be less (lower absolute value) in a real situation with non-zero permeabilities for sodium and chloride. The measured temperature gradient of the membrane potential was much higher ($-1{\cdot}30$ mV °C^{-1}, see above), which implies that a redistribution of the relative contribution of partial ionic conductances might occur during cooling.

For a simplified situation, in which only potassium and sodium conductances contribute to the resting membrane potential, eqn (2) for dependence of the membrane potential on temperature is reduced to:

$$V_m(T) = \frac{-0{\cdot}35P_K + 0{\cdot}31P_{Na}}{P_K + P_{Na}} Tm.$$

From this equation the dependence of the ratio between partial potassium and sodium conductances on temperature is described as follows:

$$\frac{P_K}{P_{Na}} = \frac{0{\cdot}31\,Tm - V_m(T)}{0{\cdot}35Tm + V_m(T)}. \quad (3)$$

Using this equation and experimental data on membrane potential we calculated the P_K/P_{Na} ratio for different temperatures (Fig. 3*D*). The ratio was strongly and highly significantly ($P < 0{\cdot}001$) correlated with temperature. Further, the mean K^+/Na^+ conductance ratios in any pair of the three selected temperature ranges were significantly different (Fig. 3*D*). From the K^+/Na^+ conductance ratio and the total membrane conductance (Fig. 3*C*), partial membrane conductance for K^+ and for Na^+ can be calculated. Partial K^+ conductance changed significantly with temperature, as indicated by a positive correlation between the two parameters and a significant difference between the mean values of partial K^+ conductances at low *vs.* high temperatures (Fig. 3*E*). At the same time, partial membrane conductance for Na^+ was essentially

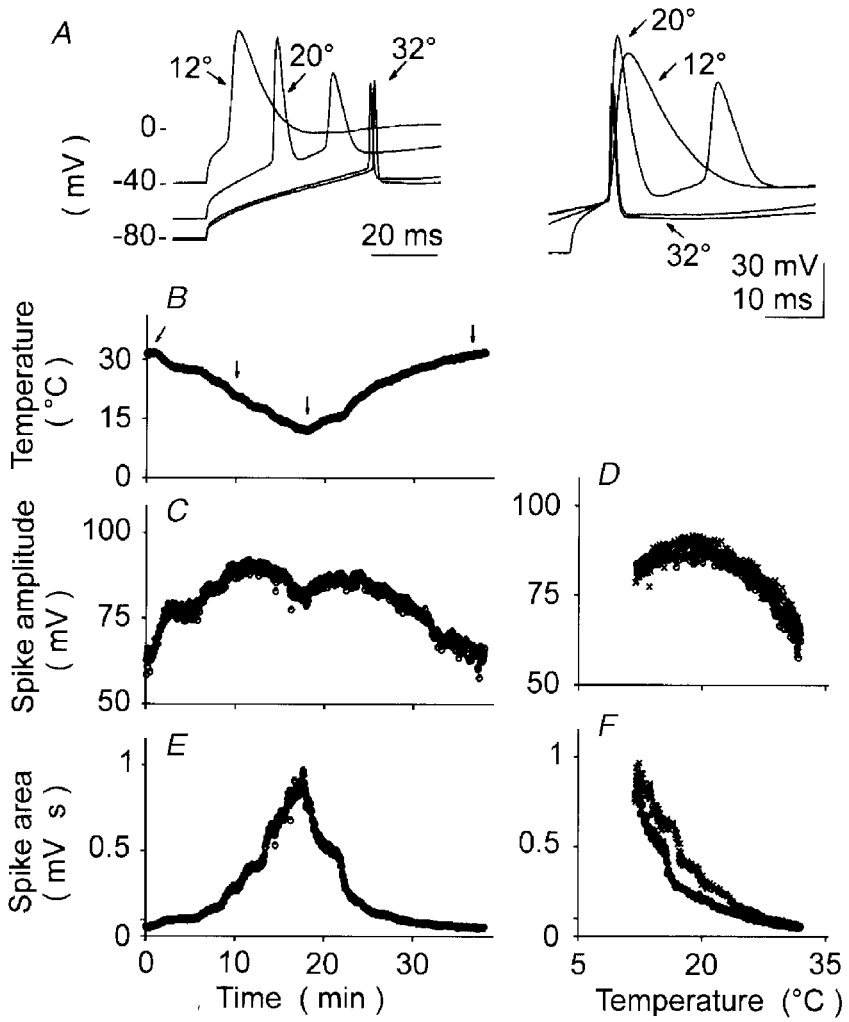

Figure 4. Dependence of spike amplitude and area on temperature in a layer 3 pyramidal cell

A, right, responses of the cell to injection of current steps (0·3 nA, 100 ms) at different temperatures (°C). At 32 °C, one trace shows the response recorded before cooling, and the other trace shows recovery after re-warming. On the left are the same responses, but aligned at the origin of the spikes. *B*, *C* and *E*, time course of changes of temperature (*B*) in the recording chamber, spike amplitude (*C*) and integral spike area (*E*). *D* and *F*, scatter diagrams showing dependence of spike amplitude and area on temperature, respectively. Values obtained during cooling are shown as crosses; those during re-warming are shown as filled circles.

independent of temperature. There was neither a significant correlation nor a significant difference between mean values for different temperature ranges (Fig. 3*F*). Hence, changes in the total membrane conductance with temperature are due mostly to changes in the partial K^+ conductance, which decreases with cooling.

If we take the chloride conductances into consideration, the situation becomes slightly more complex. It precludes quantitative calculation of the partial ionic conductances, but it does not influence the general conclusion. In theory, the cooling-induced changes of the membrane potential and of total membrane conductance that we observed could be accounted for by a disproportionately high increase of the partial chloride conductance, along with decreases of both potassium and sodium conductances that keep the K^+/Na^+ conductance ratio constant. However, our numeric simulations (data not shown) demonstrated that in such a case the absolute membrane conductance for chloride ions should increase drastically with cooling, which is highly unlikely in the light of increasing input resistance.

Therefore, we consider the decrease of the relative contribution of the potassium conductance to the total membrane conductance at lower temperatures to be the primary factor that determines the observed dependencies of the membrane potential and resistance on temperature.

Active membrane properties

Regenerative membrane conductances were activated by applying suprathreshold current pulses or steps of the holding potential. We evaluated spike amplitude and shape, spike adaptation, threshold of activation of voltage-dependent sodium channels and isolated sodium and potassium whole-cell currents. Most of these parameters changed with lowering of the temperature, and all of the observed changes recovered upon re-warming.

Spike amplitude and shape. Spikes were evoked by application of suprathreshold current steps while changing the temperature in the recording chamber. The amplitude

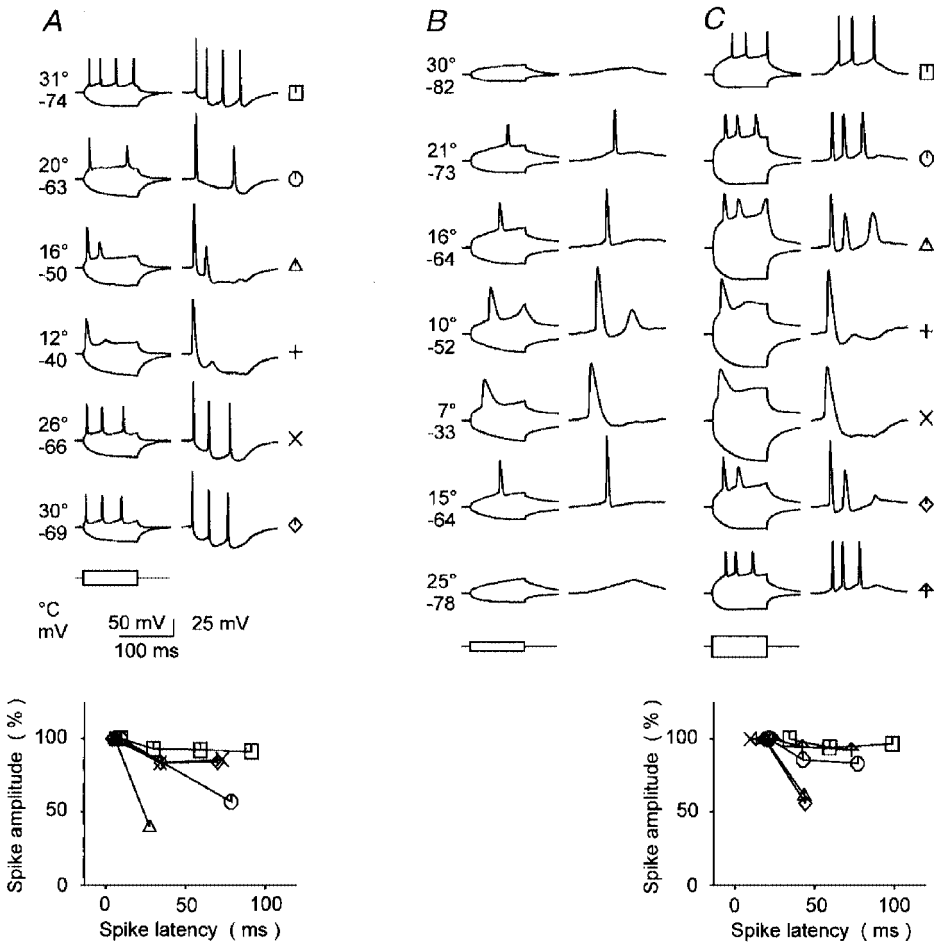

Figure 5. Temperature effects on spike adaptation

A, responses of a layer 4 spiny stellate cell to current steps at different temperatures. Responses to positive and negative current steps of the same amplitude (±0·24 nA) are shown on the left, and their algebraic sum at twice enlarged amplitude resolution on the right. Temperature and membrane potential values are indicated to the left for each pair of traces. Symbols to the right of the traces (also in *C*) code for data obtained at different temperatures for the graph at the bottom. Bottom, spike amplitude, normalized to the amplitude of the first spike in a train, plotted against spike latency, measured from the beginning of the current pulse. Values for a given temperature are connected with a line. *B* and *C*, responses of a layer 2–3 pyramidal cell to current steps (±0·15 nA in *B* and ±0·36 nA in *C*) at different temperatures. Temperature and membrane potential values indicated in *B* also refer to *C*. Other conventions and calibration as in *A*.

and shape of the spikes changed strikingly during cooling (Fig. 4). With cooling from 32 to 20 °C the amplitude, measured from the spike origin to its peak, increased by more than one-third, from 64 to 90 mV. The growth of the peak amplitude was accompanied by extension of its width from 1·3 to 5·1 ms, as measured at 15 mV above the spike origin (Fig. 4*A*). Lowering the temperature further down to 12 °C led to a further widening of action potentials (to 10·7 ms) but also to some reduction of the peak amplitude. All these changes were reversible, and both spike amplitude and shape recovered when the temperature was returned to the initial value (Fig. 4*B*–*F*). The maximal peak amplitude of the action potentials was observed at about 20 °C, both during cooling and during re-warming (Fig. 4*C* and *D*). In our sample of cells ($n = 14$, among them 10 pyramidal, 2 non-pyramidal and 2 unidentified cells) maximal spike amplitude was reached at temperatures between 12 and 20 °C. However, since the spike width increased continuously with lowering of the temperature, the total spike area increased with cooling throughout the whole temperature range (Fig. 4*E* and *F*). The total spike area was measured as the integral area under the curve from spike origin to the moment when the amplitude after the peak exceeded the threshold by less than 15 mV.

Spike adaptation. To study spike adaptation, the amplitude of the injected current step was adjusted to produce a train of three to five spikes at around 30 °C. Steps of this amplitude were applied during cooling and re-warming of the slice. The amplitude and latency after the beginning of the current step were measured for each spike. Changing the temperature altered both the timing and relative amplitudes of spikes within a train. Moderate cooling, from around 30 °C to about 20 °C affected spike adaptation differently. In the cell in Fig. 5*A* moderate cooling led to a decrease of the number of spikes in a train from four to two and to a marked reduction of the amplitude of the second spike. In another cell (Fig. 5*C*) similar cooling did not affect spike adaptation significantly, but the whole

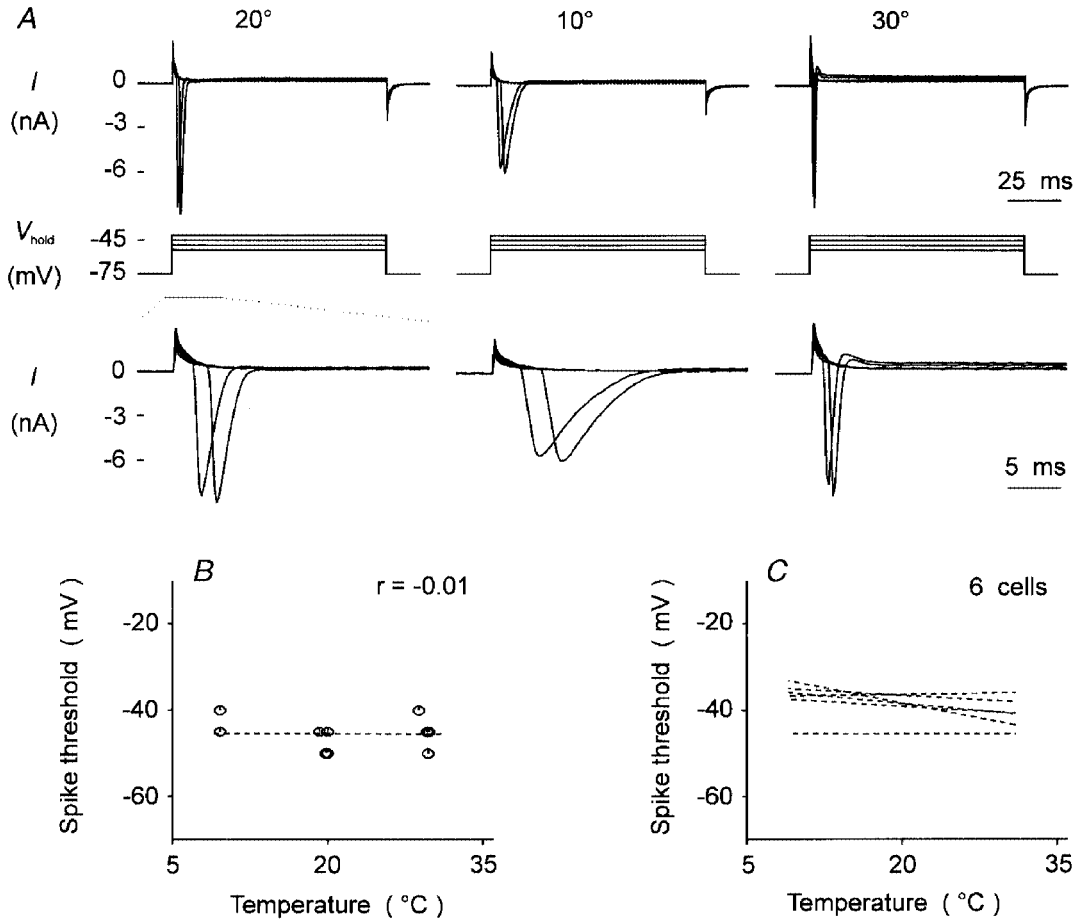

Figure 6. Stability of the threshold for spike generation at different temperatures

A, current responses (upper row) of a layer 5 pyramidal cell to step changes of the holding potential (V_{hold}) at different temperatures (as indicated, °C). Holding potential was changed from −75 mV to −55, −50, −45 and −40 mV (middle row). The initial part of the responses is shown at ×5 time resolution in the lower row. *B*, dependence of spike threshold on temperature. Each point represents the result of a single measurement of spike threshold at different temperatures (same cell as in *A*). Note that the spike threshold does not change with temperature ($r = -0{\cdot}01$). *C*, summary data from 6 cells for dependence of the spike threshold on temperature.

train of spikes occurred earlier. Cooling below 20 °C increased spike adaptation in all cells. Interspike intervals became longer, and reduction of the amplitude of consequent spikes in a train relative to the amplitude of the first spike became more pronounced (Fig. 5*A* and *C*). Remarkably, cells were capable of generating spikes even at temperatures as low as 7 °C (Fig. 5*B* and *C*). Moreover, spikes at lower temperatures were generated with progressively shorter latency (Fig. 5). This could be due to the fact that during cooling the cells got depolarized, and at the same time the input resistance increased, leading to an increase of the amplitude of the voltage shift in response to a current step of a given amplitude. This suggests that at lower temperatures a current step of a smaller amplitude is sufficient to take the cell to the threshold for spike generation. We have tested this possibility and indeed a weak current step, which was not capable of evoking spikes at temperatures above 25 °C, did lead to spikes when the temperature was 21 °C or lower (Fig. 5*B*). As in responses to the strong current pulses, a marked shortening of the spike latency occurred at lower temperatures. Interestingly, at a low temperature the cell responded similarly to strong and weak current steps, and spike responses were essentially equal (Fig. 5*B* and *C*, traces at 10 and 7 °C). Upon re-warming, the pattern of responses to current steps recovered.

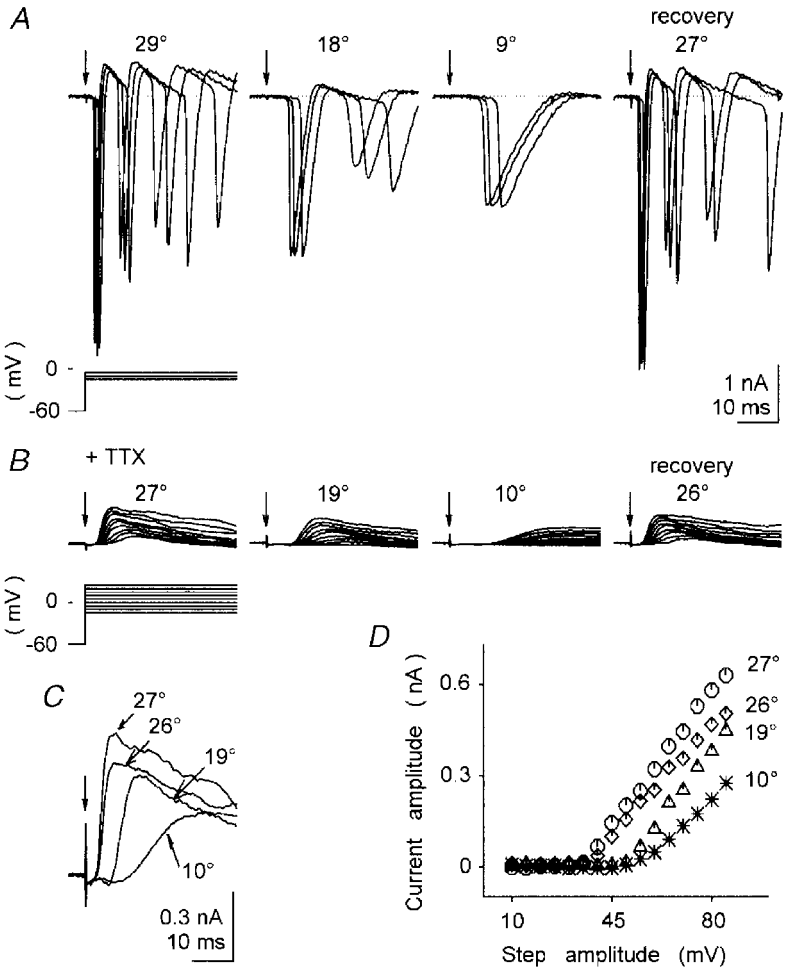

Figure 7. Current responses evoked in a layer 3 pyramidal cell by suprathreshold steps of holding potential at different temperatures during cooling and recovery

Total current (*A*) and isolated potassium current (*B* and *C*) are shown. *A*, data recorded in control medium at the indicated temperatures (°C). *B*, families of K^+ currents evoked with steps of the holding potential at different temperatures. To isolate K^+ currents, TTX (0·4 μM) was added to the extracellular medium and recording was started after all inward currents were suppressed. Data in *A*–*D* are from the same cell; the scale is the same in *A* and *B*. *C*, K^+ currents evoked with steps of the holding potential from −60 mV to 20 mV at different temperatures. Data from *B*, but at higher magnification. *D*, activation curves for K^+ currents at different temperatures, calculated from data in *B*. Note that activation threshold becomes higher at lower temperatures and recovers upon rewarming. Vertical arrows in *A*–*C* indicate the beginning of holding potential steps. Traces shown in this figure and in Fig. 8 were obtained by point-by-point summation of responses to negative and positive steps of the holding potential of the same amplitude (for example, +50 mV and −50 mV from a holding potential of −60 mV) or by using a *P*/5 subtraction protocol to exclude ohmic and capacitive components of responses.

Spike threshold. Changes of the membrane potential and input resistance associated with temperature did not permit the accurate estimation of the spike generation threshold from responses to depolarizing current steps, applied at different temperatures in the bridge mode. For this reason, we made recordings in voltage-clamp mode and applied voltage steps of different amplitudes at different temperatures. From these recordings, we could ascertain the threshold for activation of voltage-dependent sodium channels, and thus for spike generation. In the example shown in Fig. 6, steps of the holding potential to −40 mV and to −45 mV always led to spikes, while steps to −50 mV and to −55 mV did not lead to spikes at any temperature (Fig. 6*A*). Hence the threshold for spike generation was between −50 and −45 mV. Detection of the spike generation threshold was performed in this cell several times at different temperatures, and the results showed no dependence of the threshold on temperature (Fig. 6*B*). In five more cells the threshold for activation of voltage-dependent sodium channels was determined using steps of the holding potential with an increment of 5 or 2 mV, and in no case did the threshold change significantly with changes in temperature (Fig. 6*C*).

Spike-associated currents. One notable modification of the shape of the regenerative currents that occurred with lowering of the temperature was the disappearance of the outward afterspike component at lower temperatures (Fig. 6*A*). The outward component corresponds to the spike afterhyperpolarization in bridge mode recordings, which also disappeared reversibly during cooling (Fig. 4*A*). These observations suggest that potassium currents were impaired at low temperatures. To test this and to evaluate the temperature dependence of specific ionic currents and their role in temperature-induced changes in spike shape and amplitude, we performed experiments with isolated potassium and sodium currents.

Steps of the holding potential from −60 mV to −15, −10 and −5 mV applied at 29 °C evoked a characteristic sequence of inward–outward currents (Fig. 7*A*). Lowering the temperature in the bath led to some decrease of the amplitude and a salient widening of inward currents, accompanied by a reduction of the amplitude of outward currents and even their disappearance. After recovery of the initial state upon re-warming (Fig. 7*A*), a blocker of the voltage-activated sodium channels, tetrodotoxin (TTX),

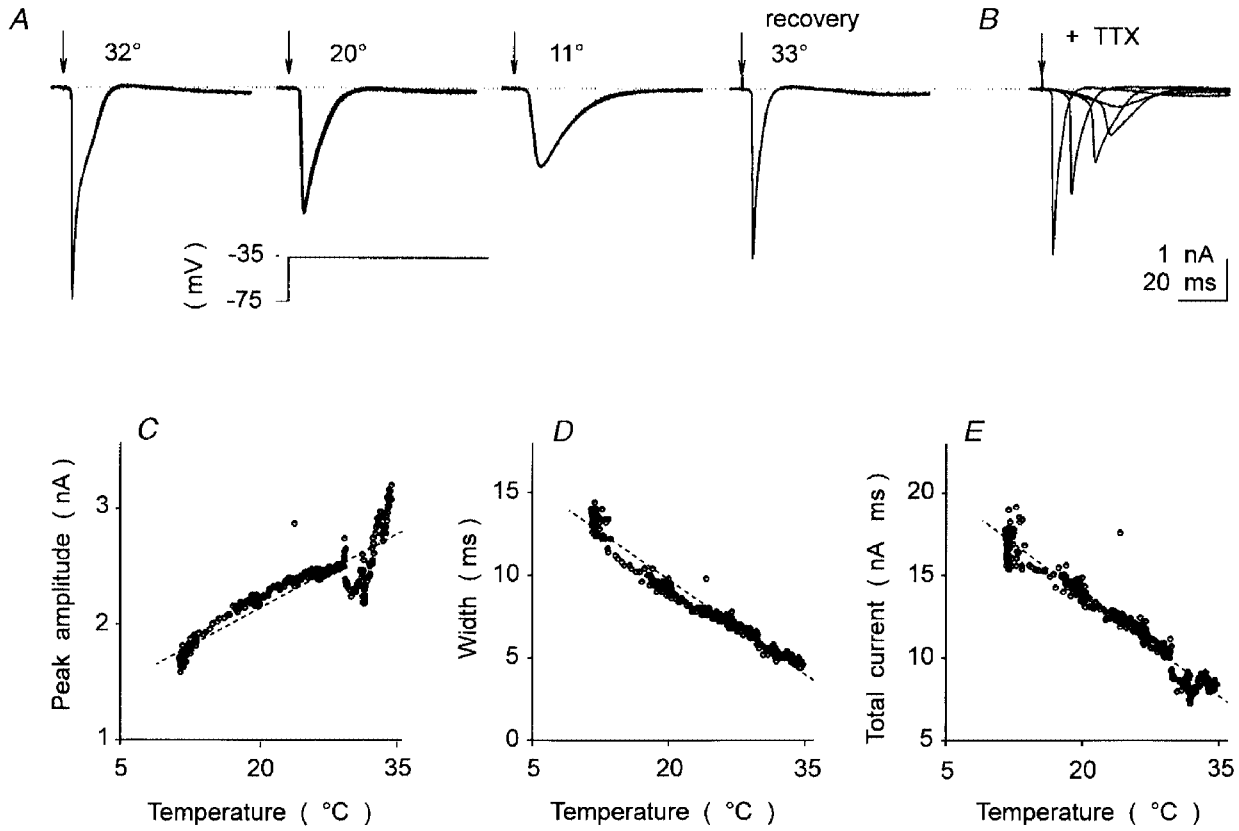

Figure 8. Temperature dependence of sodium currents evoked with steps of the holding potential

Voltage-clamp recording from a layer 3 pyramidal cell with Cs^+-based pipette solution. *A*, current responses to 40 mV steps of the holding potential. At each temperature (°C) three individual responses are superimposed. Arrows indicate the beginning of holding potential steps. *B*, suppression of sodium currents by TTX (0·3 μM). The dynamics of suppression during the first 2 min of wash is shown. *C–E*, dependence of the peak amplitude of the sodium current (*C*), its width (*D*) and integral area (total current, *E*) on temperature. Data for *A–E* are from the same cell.

was added to the recording medium. When all voltage-dependent inward conductances were blocked, families of the isolated outward whole-cell currents were recorded at different temperatures. Activation of isolated outward currents required steps of the holding potential of higher amplitude, and the stimulation protocols therefore included steps up to +25 mV (Fig. 7*B*). At 27 °C, the activation threshold of the isolated outward currents was around −20 to −15 mV. Currents induced by steps of higher amplitude had a latency approximately corresponding to the peak of the spikes and an amplitude close to the amplitude of the afterspike outward currents (compare Fig. 7*A* and *B*). Lowering the bath temperature led to an increase of the activation threshold to −10 to −5 mV, an increase of the latency and a decrease of the amplitude of the outward currents (Fig. 7*B–D*). At 10 °C, the rapid component of the outward currents disappeared, and only the slow component remained. These slow currents were unlikely to shape spikes any more since their latencies became longer than the peak latency of spikes evoked at a comparable temperature. Temperature block of the voltage-activated outward currents was reversible, and the currents recovered upon re-warming (Fig. 7*B–D*).

In the next series of experiments we studied the temperature dependence of the sodium currents. Isolated sodium currents were recorded using a Cs^+-based pipette solution. Spikes were evoked with steps of the holding potential from −75 to −35 mV, and cooling was started after all afterspike outward currents

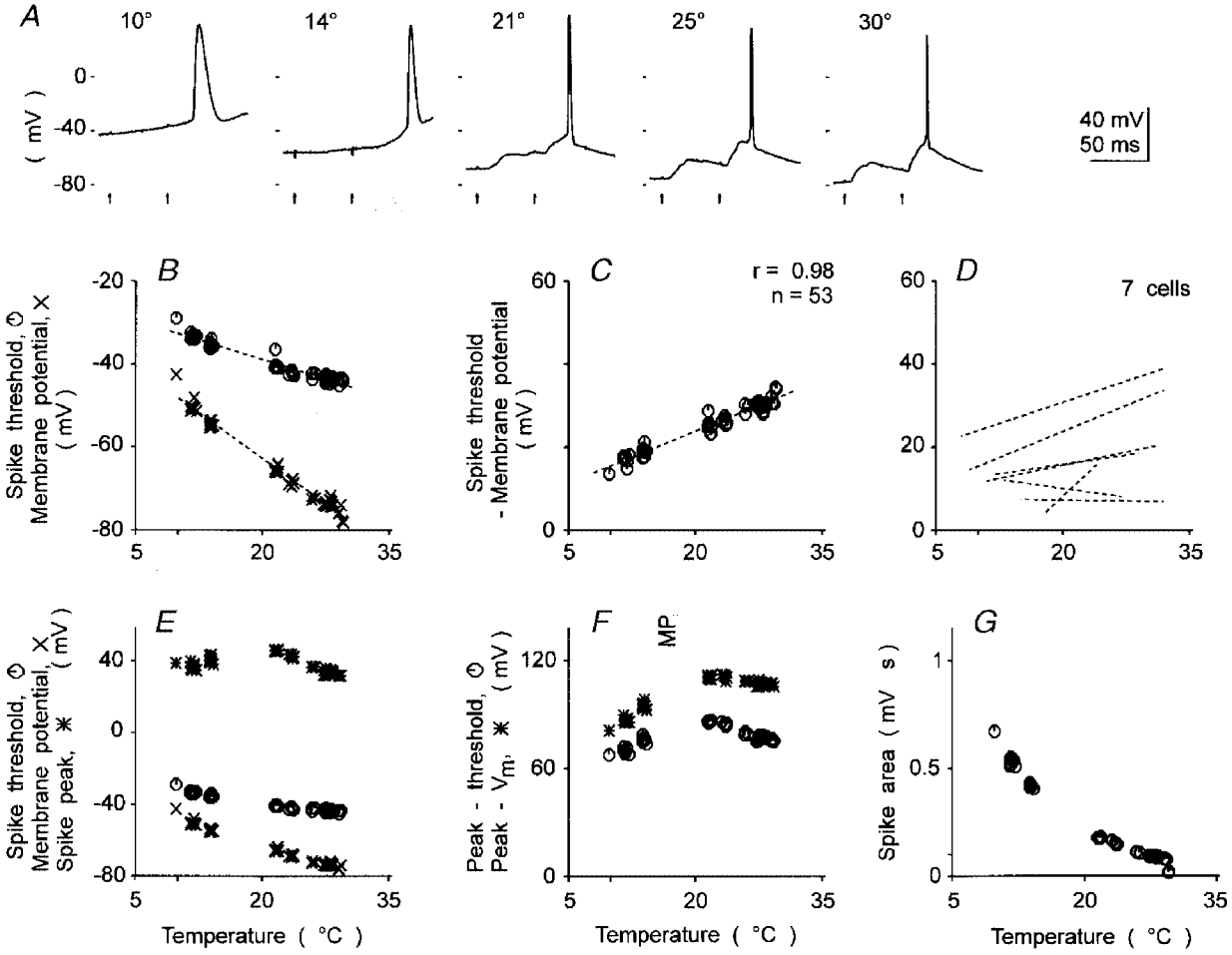

Figure 9. Effect of cooling on the threshold and amplitude of synaptically evoked spikes

A, responses evoked in a layer 2–3 pyramidal cell by a suprathreshold stimulus at different temperatures (°C). Arrows indicate application of the stimuli. *B* and *C*, dependence of the threshold of action potential generation (*B*, octagons), the resting membrane potential (*B*, crosses) and their difference (*C*) on temperature. *D*, summary data for the dependence of the difference between the threshold for spike generation and resting membrane potential on temperature. *E*, dependence of the resting membrane potential (crosses), spike generation threshold (octagons) and the potential reached at spike peak (asterisks) on temperature. *F*, temperature dependence of the action potential amplitude measured from the spike origin (octagons) and from the resting membrane potential (asterisks). *G*, dependence of spike area on temperature. Data for *A–C* and *E–G* are from the same cell.

Synaptically evoked spikes

We tested whether the temperature dependence of the characteristics of action potentials, generated in response to injection of depolarizing current steps, would also hold for spikes, evoked by synaptic stimulation. Synaptic responses were evoked by electric shocks applied through bipolar stimulation electrodes located below or lateral to the recording site. We estimated the threshold for the generation of action potentials, their amplitudes and shapes, in response to synaptic stimulation. All these parameters were temperature dependent. They changed with cooling and recovered upon re-warming.

Action potential threshold, shape and amplitude. To investigate the temperature dependence of the spike generation threshold and of the amplitude and shape of synaptically evoked spikes, we applied strong synaptic stimulation, capable of inducing spikes over a wide temperature range (Fig. 9*A*). Lowering the bath temperature led to a gradual, almost linear shift of the threshold potential from which the regenerative process started (Fig. 9*A*, and octagons in *B*). However, since cooling-induced depolarization of the cell membrane occurred with an even higher gradient (Fig. 9*A*, and crosses in *B*), the difference between the spiking threshold and the actual resting membrane potential decreased upon cooling (Fig. 9*C*). In the majority of cells (5 out of 7) tested with strong synaptic stimulation which led to spikes over a considerable range of temperatures, cooling clearly brought the membrane potential closer to the spike generation threshold (Fig. 9*D*). In one of the two remaining cells the difference between the spiking threshold and the resting membrane potential remained unchanged, and in the other cell, it slightly increased at lower temperatures (Fig. 9*D*).

The amplitude and shape of the synaptically evoked action potentials were also temperature dependent. With moderate cooling (above 20 °C) the spike peak reached more positive values (Fig. 9*E*, asterisks). The increase of the overshoot was accompanied by an increase of the amplitude of the action potentials (Fig. 9*F*) with a maximum around 21 °C. Further cooling led to a decrease of the spike amplitude due to both a decreased overshoot and a depolarizing shift of the resting membrane potential and spike threshold (Fig. 9*E* and F). The width of the action potentials increased monotonically with cooling, from 1·2 ms at 30 °C to 8·3 ms at 14 °C and to > 10 ms at 10 °C. This pronounced broadening of spikes dominated over a modest decrease of their amplitude, thus leading to a dramatic increase of the total area of the action potentials upon cooling (Fig. 9*G*). These changes are similar to temperature effects on the amplitude and shape of action potentials evoked with depolarizing current steps (see Fig. 4). Notably, synaptic stimulation could still lead to the generation of spikes even at temperatures as low as 10 °C.

Limited data from two layer 2–3 pyramidal cells recorded in slices of cat visual cortex were similar to the results described above for the rat neurones. During cooling of the

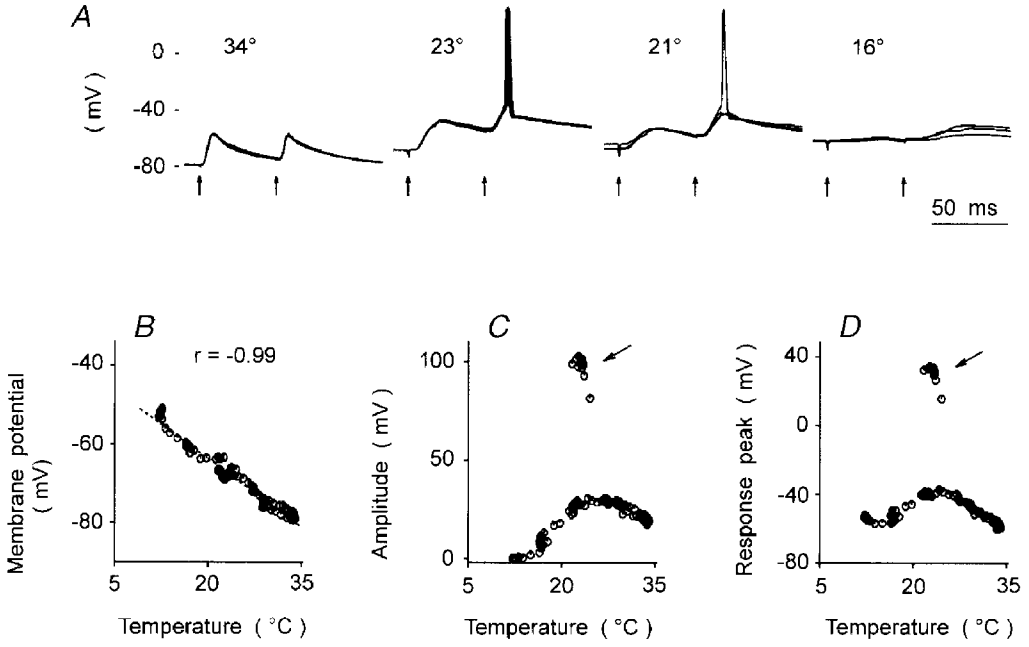

Figure 10. Subthreshold synaptic stimulation of a cat cortical neurone becomes suprathreshold during moderate cooling

A, responses evoked in a cat layer 2–3 pyramidal cell by stimuli of a constant intensity at different temperatures (°C). Stimuli were applied as paired pulses with a 50 ms interpulse interval (arrows). *B–D*, dependence of the resting membrane potential (*B*), the response amplitude (*C*) and the potential reached at the response peak (*D*) on temperature.

cat cells, we also observed a depolarization shift of the membrane potential, an increase of the input resistance and a decrease of the amplitude of the current step necessary for evoking a spike.

Hyperexcitability during moderate cooling. The above data suggest that moderate cooling to temperatures around 20 °C might lead to hyperexcitability of neocortical cells. To address this issue we adjusted the stimulus intensity to evoke EPSPs with an amplitude of 15–25 mV at around 30 °C and then continuously changed the bath temperature while applying test stimuli of that intensity. Figure 10 shows the results obtained for a layer 2–3 pyramidal cell recorded in a slice of the cat visual cortex. Synaptically evoked responses were subthreshold at 34 °C. The amplitude of synaptic responses slightly increased with lowering of the temperature down to 30 °C, and changed little with further cooling to 25 °C, but the responses remained subthreshold (Fig. 10*A* and *C*). However, since the membrane potential of the cell strongly depended on temperature (Fig. 10*B*), the EPSP peak reached higher values at lower temperatures. At 21–23 °C the depolarization potential at the peak of the EPSP response was maximal, occasionally exceeding spike threshold and thus leading to the generation of action potentials (Fig. 10*A* and *D*). With further cooling, the spikes disappeared. The EPSP amplitude recovered upon re-warming, but because of the fast recovery of the membrane potential the responses were again well below spike threshold (data not shown).

Hyperexcitability during moderate cooling was observed in six more cells recorded in slices of rat visual cortex, including one non-pyramidal cell from layer 4 and one layer 5 pyramidal cell. An increase of the EPSP amplitude during initial cooling was apparent in two of these six cells. However, even in the remaining four cases in which the EPSP amplitude did not increase, the EPSP peak reached more depolarized potentials at lower temperatures because of the high gradient of dependence of the membrane potential on temperature. The tendency of EPSPs to peak at more depolarized potentials at lower temperatures was also clearly present in nine out of ten cells in which the temperature dependence of subthreshold synaptic responses of 1–4 mV amplitude was studied (data not shown).

Altogether, hyperexcitability during moderate cooling was observed in seven cells recorded in visual cortical slices of rats and cats. In all these cells synaptic stimulation that was subthreshold at lower and higher temperatures, led to reliable action potential generation at temperatures between 18 and 24 °C.

DISCUSSION

The results of this study demonstrate that basic biophysical properties of the membranes of neocortical cells undergo marked changes during cooling, but recover rapidly and completely upon re-warming. The key factor responsible for these changes seems to be a difference in the temperature sensitivity of potassium and sodium channels. Cooling, while severely disturbing the functioning of potassium channels, has a less pronounced effect on sodium channels, thus dramatically modifying the ratio between potassium and sodium conductances. This causes an alteration of passive membrane properties, an increase in excitability of neurones, broadening of action potentials and bidirectional changes in repetitive firing. These changes, in turn, cause modification of synaptic transmission and lead to hyper-excitability of neurones in response to synaptic stimuli applied at room temperature.

Temperature effects on membrane properties and spike-associated currents

Our data show that reversible depolarization of the cell membrane, increase of the input resistance, and increase of the amplitude and width of the action potentials during moderate cooling reported earlier for cat spinal motoneurones *in vivo* (Klee *et al.* 1974) and for CA1 pyramidal cells *in vitro* (Thompson *et al.* 1985; Shen & Schwartzkroin, 1988) might be attributed mainly to a reduction of partial potassium conductance.

Some of these dependencies are similar to those described for invertebrates or lower vertebrates at temperatures below 30 °C (Schoepfle & Erlanger, 1941; Hodgkin & Katz, 1949; Frankenhaeuser & Moore, 1963; Westerfield *et al.* 1978; but see Gorman & Marmor, 1970; Kirsch & Sykes, 1987). However, at higher temperatures the similarity disappears, for example a heat block of action potential propagation occurred at around 36–37 °C in a preparation of squid giant axon (Hodgkin & Katz, 1949). Thus, adaptation to a different temperature range precludes direct comparison between cell membrane properties of invertebrates, lower vertebrates and homeothermic mammals.

Analysis of the spike-related whole-cell currents suggests that increases of spike amplitude and width during cooling might be governed by two synergistic factors. First, the voltage-dependent potassium current is delayed and dramatically decreased in amplitude with cooling, and at low temperatures its rapid component virtually disappears. This accounts for the reduction and disappearance of spike afterhyperpolarization and uncovers the voltage-dependent sodium current, which now dominates in determining spike amplitude and shape. Indeed, there is hardly any difference between a total spike-associated current and an isolated sodium current at temperatures around 10 °C. Second, the voltage-activated sodium current becomes slower with cooling, its duration becomes longer and the total charge larger, although its peak amplitude decreases. These changes could be due to slower activation and inactivation kinetics of the individual sodium channels (Sah *et al.* 1988; Milburn *et al.* 1995) and/or less synchronous opening of the channels involved in spike generation.

An increase of the spike amplitude despite a decrease of the peak amplitude of the inward currents during moderate cooling could be due to the membrane capacitance. An

action potential recorded in the bridge mode at temperatures above 20 °C, when spike-associated currents are fast, most probably reflects an integral of the currents. At this stage reduction of potassium currents and increase of the total inward current with lowering of the temperature result in an increase of both amplitude and width of the action potential. With further cooling below 20 °C, when the inward currents become slow, the action potential reflects their shape more precisely and its amplitude slightly decreases while the width continues to increase, in parallel with decreasing amplitude and increasing duration of the inward current.

Spike generation and repetitive firing

Reduction of the activity of potassium channels upon cooling and the related depolarization of the membrane potential and increase of input resistance facilitated spike generation, thus leading to hyperexcitability of cells (see below). At the same time, cooling also strengthens those factors which hinder generation of repetitive spikes. An increase of the total spike-associated inward current might increase the number of voltage-dependent sodium channels that get into an inactivated state during spike generation. Deinactivation of these channels might be delayed because of reduced afterhyperpolarization and a slowing of single channel kinetics (Sah *et al.* 1988). These factors would reduce the number of channels available for the generation of further spikes. As a result, repetitive firing of a cell could be either enhanced or suppressed upon cooling, as we observed for the temperature range from 33 to 20 °C. With further cooling, the factors preventing repetitive firing dominate.

At temperatures below 20–25 °C, the amplitude of spikes within a train does not remain constant: the first spike is the largest one, while the subsequent action potentials have smaller amplitudes. This effect can also be explained by a prolonged inactivation of voltage-gated sodium channels. Another possible factor could be a reduction of the sodium concentration gradients. Although negligible at higher temperatures, it could play a role during cooling, when the total current produced by the first spike in a train increased 5- to 15-fold and functioning of the sodium pump was slowed down.

Below 13–14 °C, cells are usually capable of generating only a single spike even in response to higher current steps that lead to a train of spikes at higher temperatures. At the same time, due to increased excitability, a small current step, which was subthreshold above 25 °C, could lead to a spike at a lower temperature. As a result, the cell responds with a single spike to the injection of either a strong or a weak current, thus losing response selectivity at low temperatures.

Hyperexcitability at room temperature

With lowering of the temperature, current steps of progressively lower amplitude were sufficient to evoke spikes. Further, the stimulus intensity, which led to synaptically evoked spikes, was minimal at room temperature, and stimuli that were subthreshold at other temperatures evoked action potentials when applied at 18–24 °C. The mechanism of this hyperexcitability rests on the strong dependence of potassium channel function on temperature. A decrease of potassium conductance during cooling increases the input resistance and also leads to depolarization of the cell membrane, thus bringing the cell closer to spike generation threshold. The absolute value of the activation threshold of voltage-dependent sodium channels does not change when the membrane potential is clamped, or may change a little as a secondary effect of depolarization. Since on moderate cooling the amplitude of evoked EPSPs decreases or increases only a little (see also Hardingham & Larkman, 1998), less excitatory input might be sufficient to evoke spikes.

One possible consequence of hyperexcitability *in vitro* could be amplification of the effect of tetanic stimulation at room temperature. Together with several additional synergistic factors, such as larger Ca^{2+} influx due to broader spikes (Borst & Sakmann, 1998) and easier removal of the Mg^{2+} block of NMDA receptors due to membrane depolarization, it could result in lowering of the threshold for induction of plastic changes of synaptic transmission. A weak tetanus, ineffective at higher, more physiological temperatures, could become just strong enough to induce plasticity at room temperature. Results consistent with this conjecture were indeed obtained in a study of the temperature dependence of the effects of tetanic stimuli that induce plastic changes in the hippocampus (McNaughton *et al.* 1994). The authors report that a weak tetanus led to much stronger potentiation when applied at 23 °C as compared to 32 °C and explain this phenomenon by changes in the excitability of presynaptic fibres induced by weak tetanization at room temperature. Our results provide another plausible explanation for their results, namely, that the same tetanus had a stronger total effect on the postsynaptic cells at room temperature. It also accounts for the otherwise unexplained block of the subnormal increase of the response amplitude by bath application of NMDA receptor antagonists at 22 °C.

The increase of the amplitude of population spikes and field EPSPs in the hippocampus *in vivo* during cooling by several degrees below body temperature (Moser *et al.* 1993; Erickson *et al.* 1996) shows that hyperexcitability upon moderate cooling is also apparent under *in vivo* conditions.

Implications for *in vitro* studies

Our data show that even the basic properties of the cell membrane and synaptic transmission at room temperature (20–24 °C) are very different from those at temperatures higher than 30 °C, stressing the necessity for taking the temperature factor into account when comparing and evaluating *in vitro* data. Assessment of the temperature dependence of membrane properties and synaptic transmission provides a basis for extrapolation of conclusions drawn from the data obtained at room

temperature to the physiological temperature range. The data also point to specific areas of interpretation where caution is necessary, for example when speculating on physiological roles of potassium conductances and currents, which are dramatically affected by temperature.

A temperature change from above 30 °C to 20–24 °C modifies a number of factors, which could affect synaptic transmission in opposite directions. At room temperature, synaptic transmission might be facilitated due to enhanced excitability of cells and fibres, increased amplitude of action potentials in presynaptic fibres, and a larger Ca^{2+} surge (Borst & Sakmann, 1998). At the same time, the slower biochemical reactions may result in an increased threshold for transmitter release (Hardingham & Larkman, 1998). A combination of slower kinetics of transmitter diffusion, uptake and binding to the receptors (Kullmann & Asztely, 1998) and slower channel dynamics may lead to either an increase or a decrease of the postsynaptic currents. Finally, depolarization of the membrane potential decreases the driving force for EPSPs, but at the same time it increases the chances for amplification of the response by NMDA receptor-mediated (Nowak *et al.* 1984; Jones & Baughman, 1988; Thomson *et al.* 1988; Sutor & Hablitz, 1989; McNaughton *et al.* 1994) or other voltage-dependent mechanisms (Huguenard *et al.* 1989; Deisz *et al.* 1991; Magee & Johnston, 1995; Schwindt & Crill, 1995; Stuart & Sakmann, 1995). A combination of these factors could lead to a net change in either direction, and indeed we have observed both increases and decreases of the EPSP amplitude during moderate cooling. The balance between the factors changes with temperature, leading to a non-monotonic dependence of the amplitude of synaptic responses on temperature.

Therefore, only *in vitro* data obtained at temperatures above 30 °C are directly relevant for applying the knowledge gained to questions of synaptic transmission *in vivo*. It appears complicated to use data gathered at room temperature for estimating physiological values of parameters like release probability, reliability or response amplitude. However, our results also indicate how, within limits, room temperature data could be corrected to yield values closer to physiological temperatures.

Implications for *in vivo* studies

Our results have important implications for *in vivo* studies which use cooling as a method of inactivation of specific brain regions. The mechanism of inactivation by cooling is a depolarization block, and before a complete inactivation is achieved, the cells inevitably pass through a hyper-excitability phase. Although this conclusion is based on the data from slices of rat visual cortex, several lines of evidence suggest that it might be applicable for cat cells as well. Our limited data from two cells recorded in slices of cat visual cortex are consistent with the results obtained in the rat. Klee *et al.* (1974) have reported for cat spinal motoneurones *in vivo* a depolarization of the cell membrane and an increase of the spike amplitude upon moderate cooling, which are similar to our data. Finally, results of *in vivo* experiments, obtained with a thermocouple glued to a recording electrode showed that complete inactivation is achieved only when cells are cooled below 10 °C (Michalski *et al.* 1993). These findings are also consistent with our results.

When a part of the brain is cooled *in vivo*, because of the high temperature gradients (Girard & Bullier, 1989; Lomber *et al.* 1996) the region under the cooling device is surrounded by moderately cooled tissue. If processes occurring during cooling of cat or monkey neocortex *in vivo* are similar to those we found in the present study in the rat, then the cells in these moderately cooled areas might be hyperexcitable rather than 'inactivated'. Consistent with *in vivo* results (Girard & Bullier, 1989; Michalski *et al.* 1993), we observed complete inactivation only when cells were cooled well below 10 °C. This implies that cooling the plate to around 9–10 °C might result in a complicated pattern of mixed effects on cortical activity. With the temperature gradients measured for the visual cortex of the cat (Lomber *et al.* 1996) and monkey (Girard & Bullier, 1989), silencing of some cells but hyperexcitability of some others is expected even within 1–2 mm from the cooling plate. At distances more than 2 mm from the plate, hyperexcitability would be the predominant effect. It should be noted here that we use the term hyperexcitability only to indicate that the cells are closer to spiking threshold, and that the first spike is easier to evoke. At the same time, due to the complex cooling-induced alterations of repetitive firing, the total number of spikes in a cell's response to afferent stimulation could either increase or decrease.

The picture of changes that occur in a moderately and non-uniformly cooled cortical area might be further complicated by markedly different gradients of temperature dependence of the properties of individual cells. Therefore, if the behaviour under cooling is similar in cat (or monkey) cortex to that found here in the rat, then data obtained with inactivation by cooling could lead to clear conclusions only when recording and cooling sites are well separated and sufficient cooling required to completely silence one region is achieved without significantly altering the temperature of the region under study. On the other hand, interpretation of electrophysiological data obtained with only moderate cooling of an area or from cells located within a moderately cooled region (Schwark *et al.* 1986; Ferster *et al.* 1996) is extremely complicated and unequivocal conclusions are hardly possible.

Borst, J. G. G. & Sakmann, B. (1998). Calcium current during a single action potential in a large presynaptic terminal of the rat brainstem. *Journal of Physiology* **506**, 143–157.

Chistiakova, M., Volgushev, M., Vidyasagar, T. R., Yousef, T. & Eysel, U. T. (1997). Temperature dependence of membrane properties and synaptic activation of neocortical cells *in vitro*. *Society for Neuroscience Abstracts* **23**, 1265.

Deisz, R. A., Fortin, G. & Zieglgansberger, W. (1991). Voltage dependence of excitatory postsynaptic potentials of rat neocortical neurones. *Journal of Neurophysiology* **65**, 371–382.

Dodt, H.-U. & Zieglgänsberger, W. (1990). Visualizing unstained neurons in living brain slices by infrared DIC-videomicroscopy. *Brain Research* **537**, 333–336.

Erickson, C. A., Jung, M. W., McNaughton, B. L. & Barnes, C. A. (1996). Contribution of single-unit spike waveform changes to temperature-induced alterations in hippocampal population spikes. *Experimental Brain Research* **107**, 348–360.

Ferster, D., Chung, S. & Wheat, H. (1996). Orientation selectivity of thalamic input to simple cells of cat visual cortex. *Nature* **380**, 249–252.

Frankenhaeuser, B. & Moore, L. E. (1963). The effect of temperature on the sodium and potassium permeability changes in myelinated nerve fibres of *Xenopus laevis*. *Journal of Physiology* **169**, 431–437.

Girard, P. & Bullier, J. (1989). Visual activity in area V2 during reversible inactivation of area 17 in the macaque monkey. *Journal of Neurophysiology* **62**, 1287–1302.

Gorman, A. L. F. & Marmor, M. F. (1970). Temperature dependence of the sodium-potassium permeability ratio of a molluscan neurone. *Journal of Physiology* **210**, 919–931.

Guttman, R. (1971). The effect of temperature on the function of excitable membranes. In *Biophysics and Physiology of Excitable Membranes*, ed. Adelman, W. J., pp. 320–336. Van Nostrand Reinhold Co., New York.

Hardingham, N. R. & Larkman, A. U. (1998). The reliability of excitatory synaptic transmission in slices of rat visual cortex *in vitro* is temperature dependent. *Journal of Physiology* **507**, 249–256.

Hodgkin, A. L. & Horowicz, P. (1959). The influence of potassium and chloride ions on the membrane potential of single muscle fibres. *Journal of Physiology* **148**, 127–160.

Hodgkin, A. L. & Katz, B. (1949). The effect of temperature on the electrical activity of the giant axon of the squid. *Journal of Physiology* **109**, 240–249.

Huguenard, J. R., Hamill, O. P. & Prince, D. A. (1989). Sodium channels in dendrites of rat cortical pyramidal neurones. *Proceedings of the National Academy of Sciences of the USA* **86**, 2473–2477.

Jones, K. A. & Baughman, R. W. (1988). NMDA- and non-NMDA-receptor components of excitatory synaptic potentials recorded from cells in layer V of rat visual cortex. *Journal of Neuroscience* **8**, 3522–3534.

Kirsch, G. E. & Sykes, J. S. (1987). Temperature dependence of Na currents in rabbit and frog muscle membranes. *Journal of General Physiology* **89**, 239–251.

Klee, M. R., Pierau, F. K. & Faber, D. S. (1974). Temperature effects on resting potential and spike parameters of cat motoneurons. *Experimental Brain Research* **19**, 478–492.

Kullmann, D. M. & Asztely, F. (1998). Extrasynaptic glutamate spillover in the hippocampus: evidence and implications. *Trends in Neurosciences* **21**, 8–14.

Lomber, S. G., Payne, B. R. & Cornwell, P. (1996). Learning and recall of form discriminations during reversible cooling deactivation of ventral-posterior suprasylvian cortex in the cat. *Proceedings of the National Academy of Sciences of the USA* **93**, 1654–1658.

McNaughton, B. L., Shen, J., Rao, G., Foster, T. C. & Barnes, C. A. (1994). Persistent increase of hippocampal presynaptic axon excitability after repetitive electrical stimulation: dependence on NMDA receptor activity, NO synthase, and temperature. *Proceedings of the National Academy of Sciences of the USA* **91**, 4830–4834.

Magee, J. C. & Johnston, D. (1995). Synaptic activation of voltage-gated channels in the dendrites of hippocampal pyramidal neurones. *Science* **268**, 301–304.

Michalski, A., Wimborne, B. M. & Henry, G. H. (1993). The effect of reversible cooling of cats primary visual cortex on the responses of area 21a neurons. *Journal of Physiology* **466**, 133–156.

Milburn, T., Saint, D. A. & Chung, S. H. (1995). The temperature dependence of conductance of the sodium channel: implications for mechanisms of ion permeation. *Receptor Channels* **3**, 201–211.

Moser, E., Mathiesen, I. & Andersen, P. (1993). Association between brain temperature and dentate field potentials in exploring and swimming rats. *Science* **259**, 1324–1326.

Neher, E. & Sakmann, B. (1983). Single channel recording. In *Single Channel Recording*, ed. Sakmann, B. & Neher, E., pp. 503. Plenum Press, New York.

Nowak, L., Bregestovski, P., Ascher, P., Herbet, A. & Prochiantz, A. (1984). Magnesium gates glutamate-activated channels in mouse central neurones. *Nature* **307**, 462–465.

Payne, B. R., Lomber, S. G., Villa, A. E. & Bullier, J. (1996). Reversible deactivation of cerebral network components. *Trends in Neurosciences* **19**, 535–542.

Sah, P., Gibb, A. J. & Gage, P. W. (1988). The sodium current underlying action potentials in guinea pig hippocampal CA1 neurones. *Journal of General Physiology* **91**, 373–398.

Schoepfle, G. M. & Erlanger, J. (1941). The action of temperature on the excitability, spike height and configuration, and the refractory period observed in the responses of single medullated nerve fibers. *American Journal of Physiology* **134**, 694–704.

Schwark, H. D., Malpeli, J. G., Weyand, T. G. & Lee, C. (1986). Cat area 17.II. Response properties of infragranular layer neurons in the absence of supragranular layer activity. *Journal of Neurophysiology* **56**, 1074–1087.

Schwindt, P. & Crill, W. E. (1995). Amplification of synaptic current by persistent sodium conductance in apical dendrite of neocortical neurones. *Journal of Neurophysiology* **74**, 2220–2224.

Shen, K. & Schwartzkroin, P. A. (1988). Effects of temperature alterations on population and cellular activities in hippocampal slices from mature and immature rabbit. *Brain Research* **475**, 305–316.

Stuart, G. & Sakmann, B. (1995). Amplification of EPSPs by axomatic sodium channels in neocortical pyramidal neurones. *Neuron* **15**, 1065–1076.

Stuart, G. J., Dodt, H. U. & Sakmann, B. (1993). Patch-clamp recordings from the soma and dendrites of neurons in brain slices using infrared video microscopy. *Pflügers Archiv* **423**, 511–518.

Sutor, B. & Hablitz, J. J. (1989). EPSPs in rat neocortical neurones *in vitro*. II. Involvement of *N*-methyl-D-aspartate receptors in the generation of EPSPs. *Journal of Neurophysiology* **61**, 621–634.

Thomson, A. M., Girdlestone, D. & West, D. C. (1988). Voltage-dependent currents prolong single-axon postsynaptic potentials in layer III pyramidal neurones in rat neocortical slices. *Journal of Neurophysiology* **60**, 1896–1907.

Thompson, S. M., Masukawa, L. M. & Prince, D. A. (1985). Temperature dependence of intrinsic membrane properties and synaptic potentials in hippocampal CA1 neurons *in vitro*. *Journal of Neuroscience* **5**, 817–824.

Volgushev, M., Chistiakova, M. & Singer, W. (1998). Modification of discharge patterns of neocortical neurones by induced oscillations of the membrane potential. *Neuroscience* **83**, 15–25.

Westerfield, M., Joyner, R. W. & Moore, J. W. (1978). Temperature-sensitive conduction failure at axon branch points. *Journal of Neurophysiology* **41**, 1–8.

Acknowledgements

We are grateful to Mrs Christa Schlauss for excellent technical assistance, to Dr Zoltan Kisvarday for help with morphology and to Drs Pavel Balaban, Thomas Mittmann and Joachim Pernberg for critically reading an earlier version of the manuscript. This work was supported by grants Ey 8/23 and SFB 509 TP A5 from the Deutsche Forschungsgemeinschaft. T.R.V. was supported by a travel fellowship from the SFB 509 and the Australian Research Council.

Corresponding author

M. Volgushev: Ruhr-University Bochum, Department of Neurophysiology, MA 4/149, D-44780 Bochum, Germany.

Email: maxim@neurop.ruhr-uni-bochum.de